Reactive and Functional Polymers 182 (2023) 105460

Contents lists available at ScienceDirect

Reactive and Functional Polymers

journal homepage: www.elsevier.com/locate/react

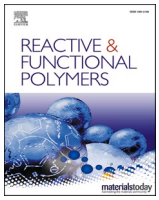

Pure aliphatic polycarbonate networks via photoinduced anionic ring-opening polymerization at elevated temperature

Stephan Schandl [a], Thomas Koch [b], Jürgen Stampfl [b], Katharina Ehrmann [a,*], Robert Liska [a]

[a] Institute of Applied Synthetic Chemistry, Technische Universität Wien, Vienna, Austria
[b] Institute of Materials Science and Technology, Technische Universität Wien, Vienna, Austria

ARTICLE INFO

Keywords:
Polycarbonate network
Cyclic carbonate monomer
Anionic ring-opening polymerization
Photopolymerization
Expanding monomer

ABSTRACT

Aliphatic polycarbonates are highly regarded due to their potential as sustainable, biodegradable and inherently biocompatible materials. Therefore, much effort has been directed towards implementation of aliphatic polycarbonates into network structures. To date, these efforts have relied on incorporation of main- or sidechain functional groups into carbonate-containing monomers or oligomeric precursors, with pure polycarbonate networks remaining inaccessible. Here we show that recently developed thermally stable photobase generators have now made cyclic carbonates available for light-induced anionic ring-opening polymerization for the first time to form pure aliphatic polycarbonate networks at elevated temperatures. To gain insights into the polymerization mechanism, the reactivity of synthesized aromatically and aliphatically substituted cyclic carbonates was investigated utilizing photo-DSC and photorheology between 70 and 120 °C. A bifunctional cyclic carbonate was synthesized as crosslinker and tested for network formation with varying amounts of the monofunctional cyclic carbonate as reactive diluent. Tensile tests and DMTA measurements revealed tough, highly tunable (thermo-) mechanical properties of the obtained materials, depending on the ratio of reactive diluent to crosslinker.

1. Introduction

Since their discovery in the early 20th century, cyclic carbonates (CC) have been investigated thoroughly regarding their reactivity during ring-opening polymerization (ROP) and ring-closing reaction, and their stability. [1–3] In recent years, CCs and their corresponding polycarbonates (PC) have been of interest due to their recyclability, [1,4] *co*-polymerizability with lactones, [5,6] as well as their potential as green alternatives for organic solvents [7,8] and for binding CO_2 during their synthesis. [8,9] Due to the biocompatibility and biodegradability [5,10,11] of aliphatic PCs, they are furthermore heavily researched in the fields of drug delivery, [12–14] macromolecular chemotherapeutics [15] and tissue engineering. [11,16]

Their polymerizability via anionic [17] and cationic [18] ROP gives rise to tailored architecture of the desired polymer. For example, including aliphatic PC blocks in polyesters, such as poly(ε-caprolactone), leads to faster and more structured hydrolysis of the polymer and increases its mechanical properties. [6,19,20] Furthermore, various applications make the synthesis of polycarbonate networks desirable. To date, this has been realized through crosslinking of carbonate-containing monomers or oligomers via additional main- or sidechain reactive groups. [21–24] However, ROP as a means to synthesize pure aliphatic carbonates is only reported for the synthesis of linear aliphatic PCs or thin films of crosslinked PC networks of low crosslinking density, [25–29] and only little is known about the photopolymerizability of cyclic carbonates via photoacid generators in cationic ROP. [30] The bimodality of the cationic ROP pathway of CCs is inevitable when using free acids as initiators. [31] The activated monomer and active chain end in cationic ROP can also be attacked by one of the endocyclic oxygen atoms of the monomer, leading to CO_2 release during ring-opening (Scheme 1). [2] This may lead to uncontrolled bubble formation and therefore limits applicability, e.g. in 3D-printing. The anionic ROP mechanism, however, does not involve activation of the carbonyl group of the cyclic carbonate. Initiated by strong organic and inorganic bases, anionic ROP proceeds as an equilibrium reaction between the CC monomer and the PC (Scheme 2). [32,33] The reaction equilibrium is influenced by the substitution pattern of the CC monomer and by the reaction temperature. [32]

The reactivity of cyclic carbonates towards ring-opening polymerization is generally low at room temperature but significantly increases with elevated temperatures. [7] Hot Lithography, with operating temperatures up to 120 °C, enables light-activated printing of resins, which

* Corresponding author.
E-mail address: katharina.ehrmann@tuwien.ac.at (K. Ehrmann).

https://doi.org/10.1016/j.reactfunctpolym.2022.105460
Received 3 October 2022; Received in revised form 21 November 2022; Accepted 24 November 2022
Available online 26 November 2022
1381-5148/© 2022 The Authors. Published by Elsevier B.V. This is an open access article under the CC BY license (http://creativecommons.org/licenses/by/4.0/).

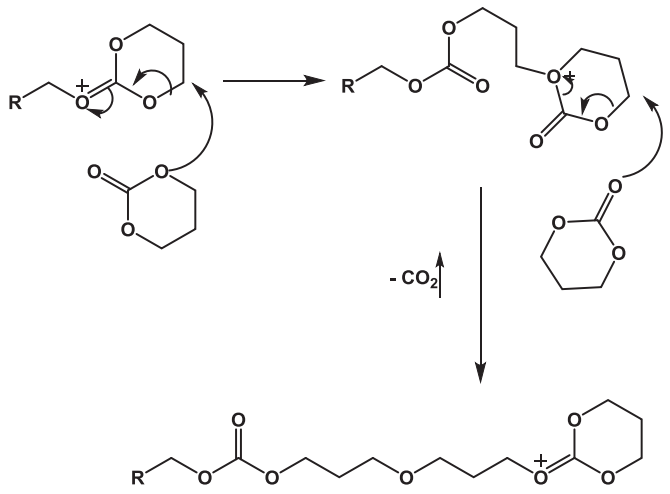

Scheme 1. Sidereaction of cROP leading to decarboxylation and formation of ether-bridged aliphatic polycarbonates. The attack of the endocyclic oxygen is favored at elevated temperatures. [7]

exhibit either too low reactivity or too high viscosity at room temperature. [34] With this technology, other moderately reactive cyclic monomers such as epoxy resins, [35,36] 2-oxazolines, [37] and lactones [38] have already been made accessible for the process via cationic ring-opening polymerization at elevated temperatures. Here we investigate the polymerizability of cyclic carbonates using anionic ROP at elevated temperatures to create pure aliphatic polycarbonate networks for the first time. The photoreactivity as well as thermal stability of mono- and bifunctional cyclic carbonates are studied in presence of a photobase generator, which is generally known to be thermally unstable [39] and may initiate the polymerization upon storage at elevated temperatures. [40,41] Finally, the (thermo-)mechanical properties are analyzed to characterize the obtained crosslinked aliphatic polycarbonates.

2. Experimental

2.1. Materials

1,1'-Carbonyldiimidazole (CDI) and 2-phenylpropane-1,3-diol were obtained from Abcr. Sodium hydroxide and THF were obtained from Acros. Ethyl acetate (EA), petroleum ether (PE), toluene and concentrated HCl were obtained from Donau Chemie. Chloroform-*d* was obtained from Eurisotop. 1,5-Diazabicyclo(4.3.0)non-5-en (DBN) was obtained from Fluka. Acetic acid, lithium aluminium hydride, 2,2-diethylpropane-1,3-diol, methyl-4-(bromomethyl)benzoate and sodium sulfate were obtained from Merck. Di(trimethylolpropane) was obtained from TCI Chemicals. All chemicals were used without any further purification.

2.2. Synthesis

2.2.1. Monomer synthesis

The synthesis of the cyclic carbonate (CC) monomers was adopted from literature. [26] Unless stated otherwise, the procedure was as follows: The precursor (1 eq) was dissolved at room temperature in 150 mL ethyl acetate. CDI (1.5 eq) was added under stirring in two portions within 5 min. After adding CDI, the reaction mixture was stirred for 30 min. Acetic acid (16 eq) was added, and the reaction mixture was heated to 75 °C for 2 h. After cooling, the reaction mixture was diluted with 150 mL ethyl acetate and washed once with 100 mL 2 N HCl. The aqueous phase was washed twice with 75 mL ethyl acetate and the combined organic phases were dried over Na_2SO_4. The organic phase was filtered and the solvent was removed under reduced pressure. Remaining acetic acid was removed via azeotropic distillation by adding 200 mL toluene. The crude products were purified by precipitation from ethyl acetate with petroleum ether. The product was filtered off, washed with petroleum ether and dried under reduced pressure.

5,5-Diethyl-1,3-dioxane-2-one (Et-C) was synthesized from 8 g (1 eq, 61 mmol) of 2,2-diethylpropane-1,3-diol and 14.7 g CDI (1.5 eq, 91 mmol). After purification, 7.6 g of the product were obtained as white crystals (80%). T_{mp}: 45.2–46.2 °C. ^{1}H NMR (400 MHz, Chloroform-*d*): δ 4.11 (s, 4H), 1.46 (q, $J = 7.6$ Hz, 4H), 0.88 (t, $J = 7.6$ Hz, 6H) ppm. ^{13}C NMR (101 MHz, Chloroform-*d*): δ 148.74, 75.06, 32.32, 22.88, 7.27 ppm.

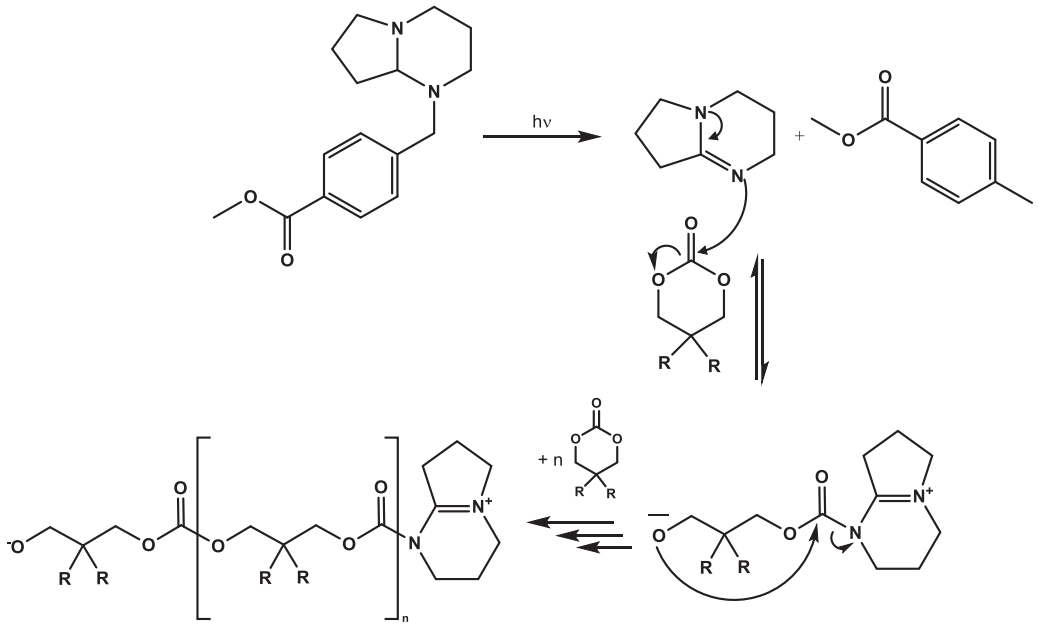

Scheme 2. Schematic reaction of photobase-initiated aROP of a cyclic carbonate. The polymer is in equilibrium with the monomer through cyclization reactions.

5-Phenyl-1,3-dioxane-2-one (Ar-C) was synthesized from 10 g 2-phenylpropane-1,3-diol (1 eq, 67 mmol) and 18.9 g CDI (1.75 eq, 113 mmol). The reaction was stirred at room temperature until a precipitate was formed. Acetic acid was added and the precipitate was redissolved. The reaction was subsequently heated to 75 °C for 2 h. The workup was performed according to the general protocol. The crude product was purified by column chromatography (PE:EA = 3:1, *v*/v) and 7.84 g Ar-C were obtained as a colorless viscous oil (66%). ^{1}H NMR (400 MHz, Chloroform-*d*): δ 7.44–7.31 (m, 3H), 7.25–7.21 (m, 2H), 4.63–4.47 (m, 4H), 3.49 (hept, J = 10.1, 5.4 Hz, 1H) ppm. ^{13}C NMR (101 Hz, Chloroform-*d*): δ 148.24, 134.09, 129.50, 128.69, 127.61, 72.18, 37.64 ppm.

5,5′-(Oxybis(methylene))bis(5-ethyl-1,3-dioxane-2-one) (Di-C) was synthesized by suspending 20 g freshly ground di(trimethylolpropane) (1 eq, 80 mmol) in ethyl acetate and adding 38.9 g CDI (3 eq, 1.5 eq per 1,3-diol functionality, 240 mmol) in two portions within five minutes. The reaction proceeded at room temperature until all starting material was consumed and all solids were dissolved. The rest of the procedure was conducted according to the general procedure. Precipitation from ethyl acetate with petroleum ether gave the purified product Di-C as colorless crystals (86%). T_{mp}: 104–105 °C. ^{1}H NMR (400 MHz, Chloroform-*d*): δ 4.22 (dd, 8H), 3.49 (s, 4H), 1.49 (q, J = 7.6 Hz, 4H), 0.91 (t, J = 7.6 Hz, 6H) ppm. ^{13}C NMR (101 MHz, Chloroform-*d*): δ 148.78, 73.26, 71.30, 35.91, 24.11, 7.84 ppm.

2.2.2. Photobase generator synthesis

Octahydropyrrolo [1,2-*a*] pyrimidine (RDBN) was synthesized via the reduction of DBN according to literature. [42] 2.5 g DBN (1 eq, 20 mmol) were dissolved in dry THF (200 mL) under argon atmosphere. Subsequently, 0.8 g of $LiAlH_4$ (1 eq, 20 mmol) were added in small portions under argon flux. The reaction mixture was heated to 80 °C for 3 h. After cooling to 0 °C, water (0.8 mL) and 15% aqueous NaOH (0.8 mL) were added and stirred for 30 min. 200 mL ethyl acetate were added, and solid contents were filtered off. Removal of the solvent gave RDBN as a yellow oil (2.36 g, 93.1%). NMR data is in accordance with data reported in literature. [43] ^{1}H NMR (400 MHz, Chloroform-*d*): δ 3.20–3.07 (m, 2H), 3.04–2.94 (m, 1H), 2.87–2.77 (m, 1H), 2.71–2.60 (m, 1H), 2.32–2.19 (m, 1H), 2.18–2.07 (m, 1H), 2.00–1.88 (m, 1H), 1.83–1.73 (m, 1H), 1.69–1.58 (m, 2H), 1.53–1.46 (m, 1H), 1.44–1.32 (m, 1H), 1.14 (s, 1H) ppm. ^{13}C NMR (101 MHz, Chloroform-*d*): δ 78.83, 51.93, 51.60, 45.70, 30.18, 26.22, 19.19 ppm.

Methyl 4-((hexahydropyrrolo [1,2-*a*] pyrimidin-1(2H)-yl) methyl)benzoate (photobase generator, PBG) was synthesized according to literature. [44] 2 g (1 eq., 15 mmol) of RDBN were added dropwise to dry toluene containing 3.63 g (1 eq, 15 mmol) of methyl 4-(bromomethyl)-benzoate. The reaction solution was stirred for 24 h, giving a suspension. The solid was filtered off, and the solvent was removed in vacuo to give the crude product. Recrystallisation in ethanol gave the product as white crystals. (1.97 g, 45%). T_{mp}: 112.5–114.3 °C. NMR data is in accordance with literature. [42] ^{1}H NMR (400 MHz, Chloroform-*d*): δ 7.96 (d, J = 8.3 Hz, 2H), 7.45 (d, J = 8.2 Hz, 2H), 3.94 (d, J = 13.8 Hz, 1H), 3.90 (s, 3H), 3.15 (d, J = 13.9 Hz, 1H), 3.13–3.02 (m, 2H), 2.85–2.79 (m, 1H), 2.45 (dd, 1H), 2.25 (q, J = 8.7 Hz, 1H), 2.15–2.06 (m, 1H), 2.06–1.96 (m, 1H), 1.93–1.83 (m, 3H), 1.81–1.61 (m, 2H), 1.54–1.43 (m, 1H) ppm. ^{13}C NMR (101 MHz, Chloroform-*d*): δ 167.27, 144.91, 129.68, 128.89, 84.77, 76.84, 58.41, 52.59, 52.44, 52.14, 51.24, 29.88, 24.81, 19.59 ppm.

2.3. Formulation and specimen preparation

Formulations were prepared by dissolving the initiator PBG (5 mol%) and the sensitizer ITX (50 wt% of PBG), in the monomer by heating and stirring. DMTA and tensile test specimens were produced by curing the formulation in silicone moulds using an Ivoclar Lumamat 100 light oven (400–580 nm) at 100 °C for 25 min. All test specimens were postcured at 120 °C overnight to ensure complete conversion. The surfaces of the test specimens were ground to unified dimensions prior to testing.

2.4. Physico-chemical characterization

2.4.1. Nuclear magnetic resonance (NMR) spectroscopy

NMR spectra were recorded on a BRUKER Avance DRX-400 FT-NMR spectrometer. Chemical shifts were indicated in ppm relative to tetramethylsilane (δ = 0 ppm) and referenced on the used NMR solvent. The multiplicity of the signals was stated as s = singlet, d = doublet, dd = doublet of doublets, t = triplet, q = quadruplet, hept = heptet, m = multiplet. Obtained spectra were analyzed using the MestReNova software by Mestrelab Research.

2.4.2. Melting point analysis

Melting intervals were measured using an automated OptiMelt device from SRS Stanford Research System.

2.4.3. Photo-DSC

Photo-differential scanning calorimetry (photo-DSC) measurements were performed in triplicates on a Netzsch DSC 204 F1 with an autosampler and a double-core glassfiber light guide (diameter: 3 mm) at 70 °C, 100 °C and 120 °C under N_2 atmosphere. An Exfo OmniCure TM 2000 device with a spectral range of 320–500 nm from Lumen Dynamics was used as irradiation source. The lamp was calibrated using an OmniCure R2000 radiometer. The light intensity was set to 50 mW cm^{-2} on the sample's surface, corresponding to 1.5 W cm^{-2} at the tip of the light guide. One measurement consisted of three segments: (1) 240 s isothermal equilibration; (2) and (3) irradiation for 300 s. Obtained results represent the heat of polymerization of the formulation as function of time. Subtraction of the second irradiation phase was performed to remove background signals during evaluation. For the evaluation of the conversion and molecular weight, two samples were dissolved in $CDCl_3$ and THF for NMR and GPC analysis, respectively. 0.3 wt% acetic acid were added to the NMR solvent to quench the reaction. The conversion was determined using the CH_2 signals adjacent to the carbonate unit (Ar-C: 4.55 ppm; poly(r-C): 4.32 ppm, Et-C: 4.12 ppm; poly(Et-C): 3.98 ppm) according to the following formula:

$$NMR-conversion\,(\%) = \left(1 - \frac{\int monomer - signal}{\int monomer - signal + \int polymer - signal}\right) * 100$$

The sum of the integrals of the monomer signal and the polymer signal was set to 4, according to 4H atoms next to the carbonate unit.

2.4.4. Gel permeation chromatography

GPC measurements were conducted on a Waters GPC with three columns in series (Styragel HR 0.5, HR 3 and HR 4) and a Waters 2410 RI detector. The measurements were evaluated using conventional calibration with polystyrene standards (in the range of 0.4–177 kDa) to determine the molecular weight of polymers. The samples were dissolved in THF (2 mg mL^{-1}, BHT as stabilizer and flow rate marker) and transferred into GPC vials via syringe filtration.

2.4.5. Photorheology

Photorheology analysis was performed on an Anton Paar MCR 302 WESP device with a P-PTD 200/GL Peltier glass plate and a PP25 measuring system. An Exfo OmniCure 2000 T.M. was used as an irradiation source. The lamp was calibrated with an OmniCure R2000 radiometer, and the light intensities were adjusted to the stated value using an Ocean Optics device. The glass plate was heated to the selected temperature, and 130 μL of formulation were placed on the plate. The stamp was lowered to a gap size of 2 mm for 1 min for formulations with a high melting point. The gap size, shear rate and strain were set to 0.2 mm, 1 Hz and 1%, respectively. After 60 s, the irradiation started for 600 s. Each formulation was measured three times. The values for the time until the gel point is reached (t_g) were determined from the point of intersection of the storage (G') and loss modulus (G") curves.

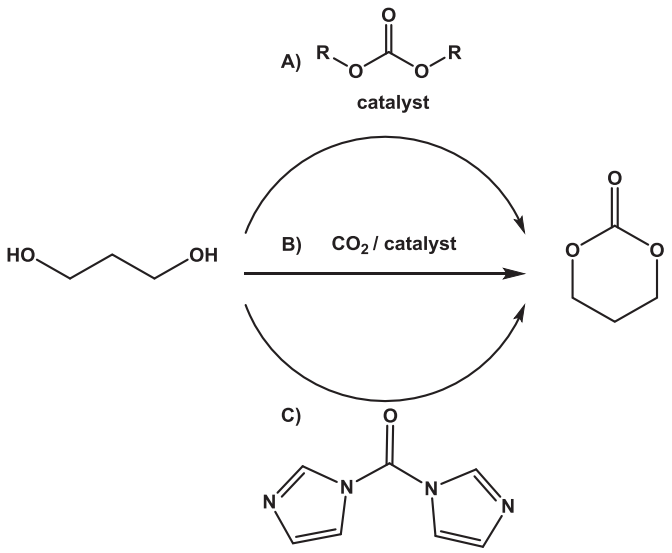

Scheme 3. The three major pathways for the synthesis of cyclic carbonates: A) Reaction of a diol-precursor with phosgene or derivatives thereof; B) reaction with CO_2 in the presence of a catalyst; C) cyclization using CDI as carbonyl source

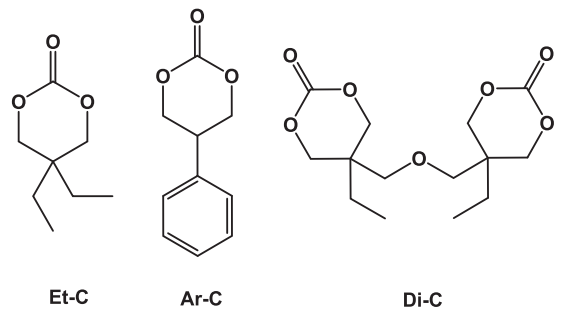

Fig. 1. Molecular structures of the investigated cyclic carbonate monomers

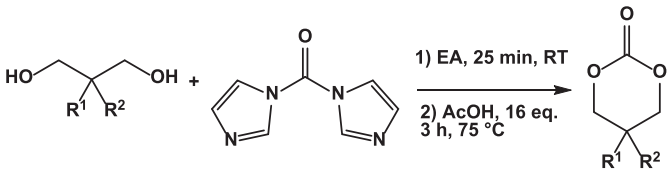

Scheme 4. Generalized reaction scheme for the synthesis of cyclic carbonates using 1,1′-carbonyldiimidazole as carbonyl source

2.4.6. Differential scanning calorimetry

DSC measurements were conducted on a T.A. Instruments DSC 2500. The formulations were weighed in and polymerized in aluminium crucibles (10–15 mg) and covered with a pierced lid. The samples were postcured at 120 °C overnight prior to testing. Two heating runs with a cooling run in between were performed with a temperature ramp of 10 °C min^{-1}. The screened temperature ranged from −50 °C to 200 °C.

2.4.7. Dynamic mechanical thermal analysis

DMTA was performed on an Anton Paar MCR 301 device with a CTC 450 oven. The test specimens had the dimensions of 5 × 2 × 40 mm^3 and were measured in torsion mode with a frequency of 1 Hz and 0.1% strain. The temperature was increased from −100 to 200C with a heating rate of 2 °C min^{-1} and the loss factor (tan δ), storage and loss modulus were recorded as a function of temperature. The glass transition temperature was defined as the temperature at the peak maximum of the loss factor. [35]

2.4.8. Tensile tests

Test specimens were prepared in the form of ISO 527 test specimen 5b (2 × 2 × 12 mm^3 parallel region, total length of 35 mm). [45] Tensile tests were performed on a Zwick Z050 tensile machine equipped with a 1 kN load sensor The samples were strained with a crosshead speed of 5 mm min^{-1}. During the measurement, a stress-strain plot was recorded for analysis. Five specimens were tested for each formulation with satisfactory reproducibility. Tensile toughness was obtained by integration of the stress-strain curves using OriginLab Software (V2019).

2.4.9. Thermogravimetric analysis

Thermogravimetric analysis was performed on a T.A. Instrument TGA Q500 under nitrogen atmosphere. The samples were weighed in, polymerized in aluminium crucibles (10–15 mg), covered with a pierced lid and postcured at 120 °C. Finally, they were analyzed with a heating ramp of 10 K min^{-1} between 30 °C and 400 °C.

3. Results and discussion

3.1. Synthesis

The synthesis of cyclic carbonates can be performed via three different reaction pathways: A) using phosgene or derivatives thereof, e.g., dimethyl carbonate, diphenyl carbonate; B) reaction with CO_2; C) reaction with 1,1′-carbonyldiimidazole (CDI) as carbonyl source (Scheme 3). While all of them are well-established procedures, the targeted bifunctional aROP monomer in this work requires special considerations for the choice of the synthetic pathway. Furthermore, application of the monomers in materials requires scalability and fairly straight forward purification methods. For pathway A, strong bases are used as catalysts and the equilibrium is shifted towards the product by either distilling off the byproduct, ethanol or methanol, [3] or exploiting the stability and low nucleophilicity of the phenolate anion. [28] However, these reactions are always accompanied by the byproduct formation of the corresponding linear polycarbonate. For example, we found for Ar-C that the linear polycarbonate seemed to be the main product from diethyl carbonate or diphenyl carbonate reactions via pathway A. While continuous distillation at high temperatures and under high vacuum could be performed to depolymerize the linear polycarbonate for monofunctional CCs, [17] CCs cannot be synthesized this way, as a crosslinked material would result from these side reactions. Furthermore, those synthetic pathways suffer from inadequate scalability and tedious purification procedures due to the high excess of reactant and due to high sensitivity towards water and other impurities of the precursor. [17] Similar sensitivity towards water, air and impurities is reported for the synthetic pathway B using CO_2 as a reagent. [8] Such reactions are mostly performed in an autoclave under high pressures of CO_2 and temperatures of up to 110 °C [8] with few exceptions at atmospheric pressure and room temperature. [46,47] Therefore, reaction pathway B was also deemed unfeasible for this work. Pathway C using CDI as carbonyl source for the synthesis of CCs [26] was successfully applied to synthesize the targeted CCs based on aliphatic 1,3-diols for mono- and bifunctional CCs (Fig. 1, Scheme 4). The results from the synthesis of Di-C imply good specificity towards the CC during the acidic hydrolysis of the intermediate. This synthesis pathway is a robust reaction with low sensitivity to water and promises freedom of substitution for all kinds of aliphatic CCs. Compared to route A using diethyl carbonate or diphenyl carbonate, higher yields were obtained with higher purity in the crude reaction product for synthesis route C. In the case of Et-C, yields of the transesterification pathway A using diethyl carbonate and diphenyl carbonate, up to 73% and 80%, respectively, were achieved compared to yields of 85% via the CDI pathway C. As scalability of the CDI pathway was more feasible due to low reaction

Table 1
Summary of the GPC and ^{1}H NMR analysis of polymers obtained from the pure reactive diluents Et-C and Et-Ar between 70 and 120 °C.

T (°C)	Conversion (%)	M_n (kDa)	DP ()	Đ ()
		poly(Et-C)		
70	30	1.4	9	1.20
100	41	1.9	12	1.18
120	30	1.9	12	1.16
		poly(Ar-C)		
70	37	3.1	17	1.20
100	75	4.4	25	1.27
120	93	4.2	24	1.37

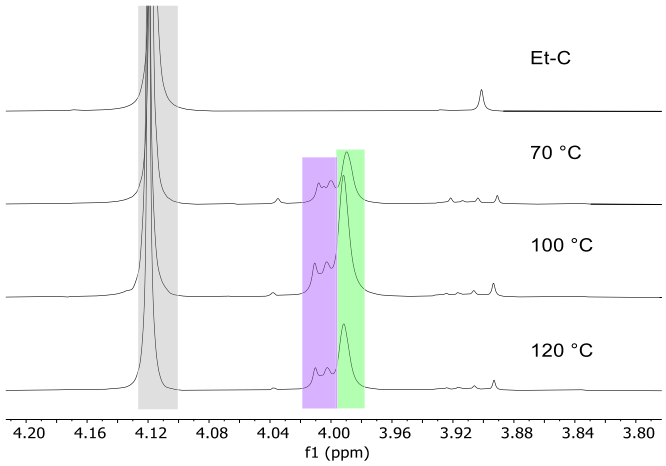

Fig. 2. NMR study of the polymerized samples from photo-DSC analyses of Et-C between 70 and 120 °C. The signals for the Et-C monomer (grey box, 4.12 ppm) and the growing polymer (green box, 3.99 ppm) show distinct differences in their chemical shifts. The starting group of the growing polymer (purple box, 4.01 ppm) can also be observed. (For interpretation of the references to colour in this figure legend, the reader is referred to the web version of this article.)

times and easy purification, this synthesis method was adapted for all monomers. Additionally, purification via column chromatography was successfully replaced by precipitation for the reactive diluent Et-C and the crosslinker Di-C, enhancing scalability. In the case of reactive diluent Ar-C, which was obtained as an oil, flash chromatography could be performed to remove oligomers and unreacted precursors.

3.2. Reactivity studies

3.2.1. Photo-DSC

Photo-DSC experiments were performed to investigate the system's reactivity towards photoinduced anionic ROP. Three formulations consisting of one of the three monomers and 5 mol% PBG were tested at 70, 100 and 120 °C. Due to the low ring-strain of six-membered rings and low reaction enthalpy hardly any polymerization heat was observed during all reactions. Therefore, the linear polymers resulting from the reactive diluents were analyzed regarding molecular weight and overall conversion via GPC and ^{1}H NMR, respectively (Table 1). The crosslinker Di-C formed networks as expected and was therefore inaccessible for these analyses. It was observed that the molecular weight increased with increasing temperature and a conversion maximum occurred at 100 °C. The conversion observed at 120 °C was lower than at 100 °C and the molecular weight was equal at both polymerization temperatures. This could be due to the nature of anionic ROP, which inherently leads to an equilibrium between the polymer and the cyclic monomer. A decreasing polydispersity index (Đ) with increasing temperature also indicates that the equilibrium could shift towards longer, more homogeneously

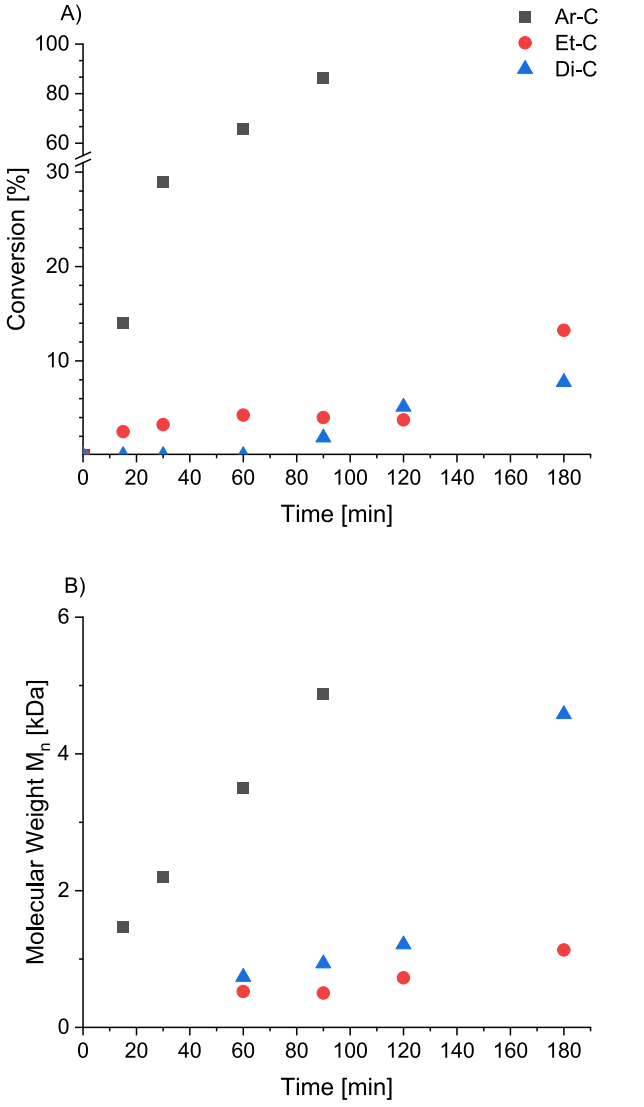

Fig. 3. Thermal stability of the formulations of each investigated monomer at 120 °C, depicted in terms of conversion (A) and number-average molecular weight M_n (B). Ar-C proved to be highly reactive and unstable over time and increased in viscosity so that after 90 min, no more samples could be drawn.

distributed chains. The ^{1}H NMR analyses of cured DSC samples from monofunctional monomers, as exemplarily depicted in Fig. 2 for Et-C, show that there are no ether-bridged units, as expected for anionic ROP. Furthermore, the presence of the starting unit of the growing polymer chain can be seen at 4.01 ppm. It can also be seen that the ratio of the growing chain to the starting unit is maximal at 100 °C and decreases at lower and higher temperatures. This is again indicative of the shift of the equilibrium of the anionic ROP towards the cyclic monomer with a narrower distribution in chain length of the polymer. The comparison of all photopolymerized monomers at 120 °C also showed that the aromatically substituted monomer, Ar-C, was more reactive than Et-C. The high reactivity explains the broader distribution of molecular weights, as indicated by a slightly higher dispersity at higher temperatures. In the case of the crosslinker Di-C, ^{1}H NMR provided no signals for residual monomers after leaching the network obtained during the photo-DSC measurement for 2 h. Therefore, it was concluded that all monomers had become part of the network.

3.2.2. Thermal stability of the formulations

Formulations containing photobase generators are usually not

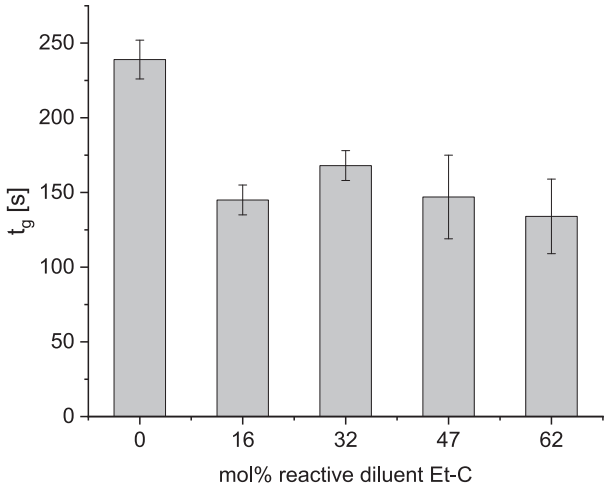

Fig. 4. Glass transition temperatures from the photorheological analysis at 110 °C for Di-C with 0–62 mol% reactive diluent Et-C.

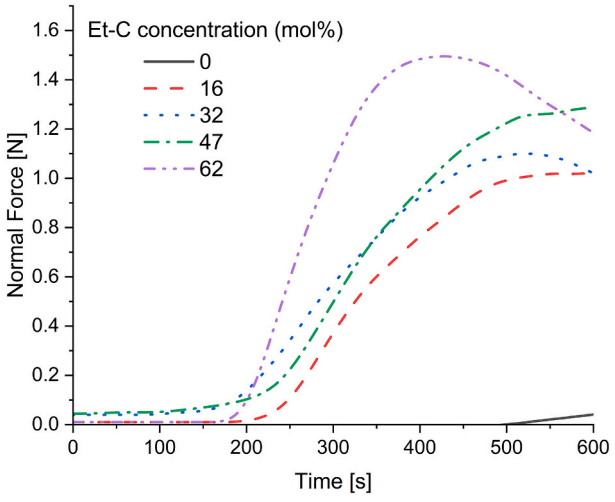

Fig. 5. Normal force as a function of irradiation at 120 °C during rheological studies proving the expanding nature of cyclic carbonates during aROP. The pure Di-C systems (0 mol% Et-C) showed the least and latest increase in normal force. This could be caused by low diffusion of the PBG through the system or steric hindrance of the side groups of the monomer.

thermally stable over a prolonged time period. Therefore, a thermal stability study was performed to assess the formulations' stabilities. The formulations were stored at 120 °C, and samples for ^{1}H NMR and GPC analysis were drawn at predetermined time points to measure conversion and molecular weight (Fig. 3). We found that the monofunctional monomer Ar-C is highly susceptible to thermal initiation by the initiator PBG and therefore not suitable for a potential printing process, which can take several hours. Therefore, this monomer was excluded from further tests. The monomer Et-C and the crosslinker Di-C proved to be relatively stable for up to 120 min with only minimal conversion and number-weighted molecular weight increase over time occurring between 120 and 180 min (Fig. 3). While Di-C proved to be fairly stable up to 120 min as well, solubility was impaired after 180 min and drastically increased molecular weight fractions were observed for the soluble fraction (Fig. 3 B).

3.2.3. Photorheology

After thorough individual examination of each monomer via photo-DSC, further reactivity tests were performed with photorheology to

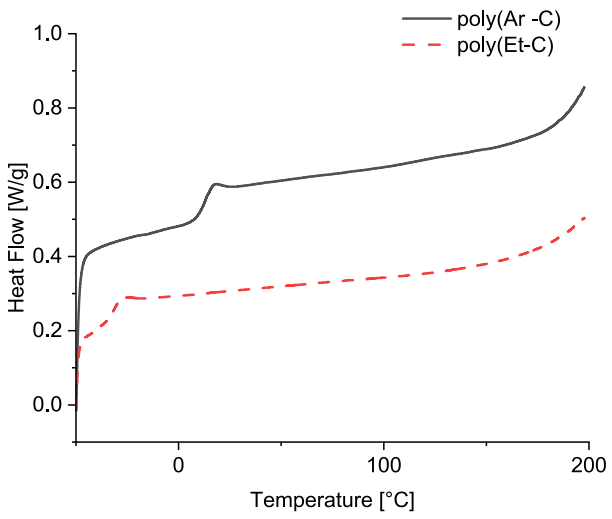

Fig. 6. DSC of the linear polymers poly(Ar-C) and poly(Et-C). The T_g of the alkyl-substituted polycarbonate was observed at −30 °C compared to the T_g at 35 °C of the aryl-substituted polycarbonate.

determine the time until the gel point (t_g) was reached for formulations of different crosslinking densities, which was realized by mixing the crosslinker Di-C with various concentrations of Et-C at 110 °C. This indicates the minimum irradiation time for a layer during printing and therefore printing speed. It was observed that t_g decreases from 240 s for the pure crosslinker to 140 s upon addition of as little as 16 mol% Et-C. However, when the Et-C concentration was further increased up to 63 mol%, the formulation showed similar times until the gel point was reached (Fig. 4) and initial G' increases were the same (Fig. S14) within the investigated range of Et-C additions. Therefore, it can be assumed that both monomers are equally reactive once the ring-opening polymerization has started. Reactive diluent concentration dependent variations in reactivity only occur at later stages of the polymerization and are therefore likely a result of impaired diffusivity of the sensitizer and PBG from a certain crosslinking density on. The recorded increased normal force of the polymerizing formulation indicates the expanding nature of CC monomers during ROP, which promises good dimensional stability and little mechanical strain of cured samples (Fig. 5). Formulations with higher concentrations of reactive diluent show higher expansion due to less steric confinement and therefore more flexible network formation. Additionally, the formulation containing 63 mol% reactive diluent has the fastest increase in normal force and exhibits a maximum around 400 s curing time. The decrease of the normal force after 400 s could be caused by unreacted resin being pushed out from underneath the stamp. Interestingly, a pure crosslinker system containing 100% Di-C shows the lowest reactivity and expansion. Two factors could be responsible for the low reactivity of the crosslinker. One is the limited diffusion of the PBG and the active species within the formulation. Another possibility for the delayed reaction could be caused by the temperature at which the measurements were performed. 110 °C at the glass plate was enough to melt Di-C (T_{mp}: 104–105 °C) but not the PBG (~115 °C). This could indicate that the pure crosslinker, in contrast to the reactive diluent, is a worse solvent for the PBG. Hence, less PBG was dissolved within the formulation during the measurements. However, due to instrumental limitations, the temperature could not be set to higher temperatures to prove this hypothesis.

3.3. Thermal and (thermo-)mechanical analysis

DSC measurements were performed for cured photo-DSC samples to characterize the materials obtained and determine the glass transition temperature (T_g) of the linear polymers obtained from Et-C and Ar-C

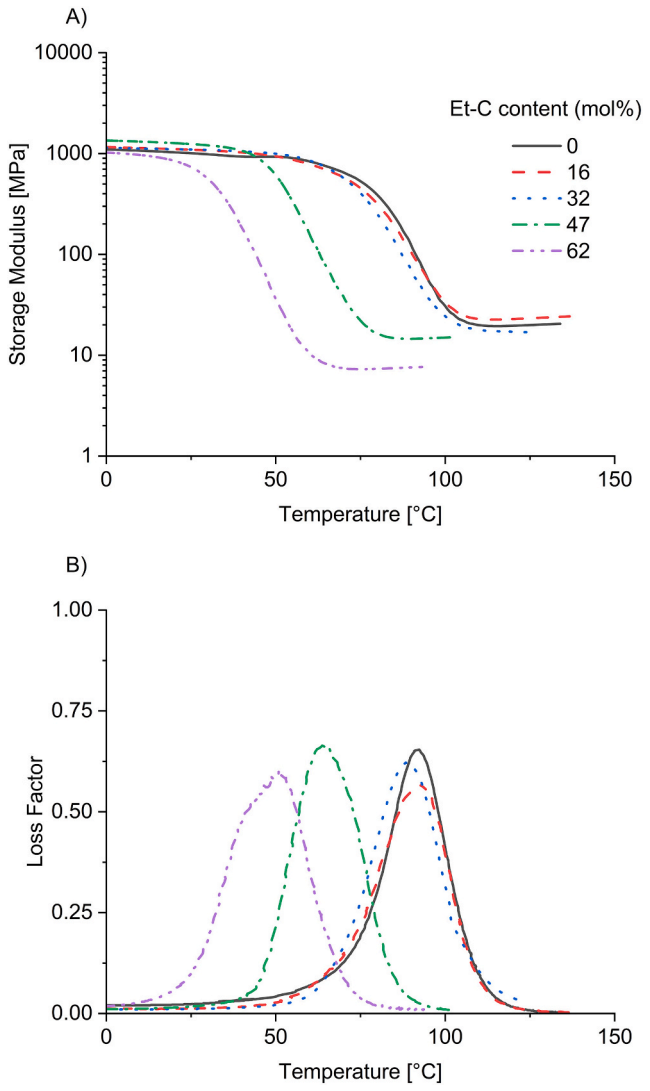

Fig. 7. Results from DMTA show the influence of the reactive diluent on T_g is not significant as long as the crosslinker is the main component of the formulation. T_gs range from 88 °C (pure Di-C and Di-C with up to 32 mol% Et-C) to 47 °C (Di-C with 62 mol% Et-C).

(Fig. 6). As expected, the influence of the side groups leads to a significant change in T_g. The aliphatically disubstituted Et-C-based polymer exhibits a T_g of −30 °C, whereas the introduction of the aryl side-group increases the T_g to 35 °C. This was also observed in their appearances at room temperature. Poly(Et-C) was a viscous liquid, whereas poly(Ar-C) was a solid and stiff material. DMTA measurements were performed to determine the T_g (Fig. 7). Adding up to 32 mol% of the reactive diluent Et-C did not alter the T_g of the material. The addition of more reactive diluent reduced the T_g from 92 °C (pure Di-C) to 47 °C (62 mol% Et-C). The large shift towards lower temperatures was caused by the low T_g of linear poly(Et-C), which lead to more flexibility within the material. The influence of Di-C to Et-C ratio on the mechanical properties can also be seen in the tensile test results (Fig. 8). With up to 32 mol% Et-C in the material, the elongation at break can be increased significantly without or with only minor decrease of maximum strain, resulting in enhanced tensile toughness. In particular, the stress-strain curve of samples containing 47 mol% Et-C exhibits a distinct yield point, which is indicative for rigid and tough materials. When the reactive diluent becomes the main component of the formulation, the elongation at break increases from 8% to 40% and the maximum stress is reduced from around 70 MPa to 12 MPa. The addition of the reactive diluent Et-C to the system

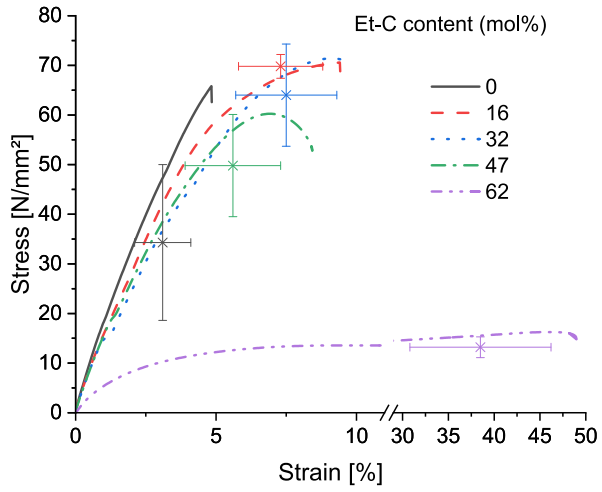

Fig. 8. Stress-strain diagram obtained from tensile testing at 25 °C, displaying the best tensile curves as well as the average stress and strain values at break. Addition of the reactive diluent Et-C up to 47 mol% improved stress and strain at break. However, as the reactive diluent becomes the dominating component of the formulation, the material properties drastically changed to a more elastomeric behavior.

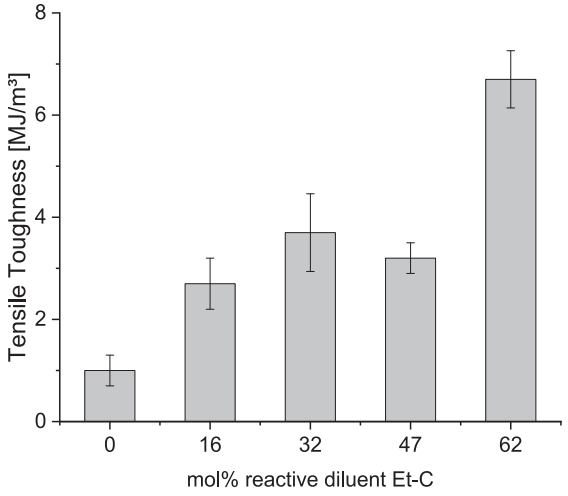

Fig. 9. Tensile toughness of the obtained materials. The addition of up to 50 mol% reactive diluent Et-C increased the tensile toughness, above 50 mol% Et-C content this increase is accompanied by a decrease of maximum yield stress.

increased tensile toughness compared to the materials obtained from pure Di-C in all cases (Fig. 9). However, the more rigid materials obtained with concentrations of up to 47 mol% reactive diluent should not be compared to the results obtained from the test specimens with 62 mol % reactive diluent, which exhibit elastomeric properties and increased tensile toughness was caused by the high elongation at break in this case. The reactive diluent Et-C also impacts the thermal stability of the crosslinked material (Fig. 10), indicated by $T_{5\%}$, which is the onset of mass loss, i.e. the temperature, where 5% of mass loss was observed. The pure crosslinker Di-C shows a $T_{5\%}$ of 257 °C, which gradually decreases with the addition of reactive diluent. The linear polymer poly(Et-C) shows a distinctively earlier onset, almost 40 °C earlier than the crosslinked materials at a $T_{5\%}$ of 216 °C.

4. Conclusion

In this study, three cyclic carbonate monomers were investigated for their potential in light-induced anionic ROP. Two different reactive

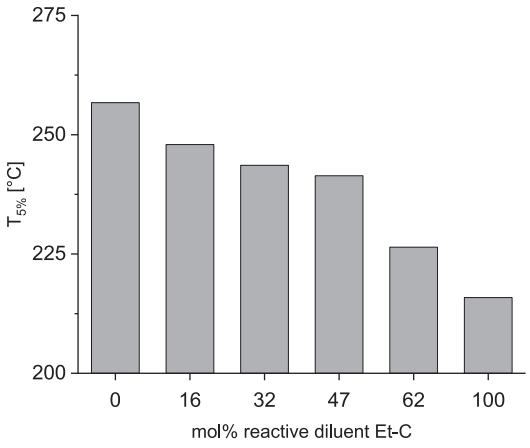

Fig. 10. Thermogravimetric analysis of the crosslinked materials (Di-C with 0–62 mol% Et-C) and linear poly(Et-C) (100% Et-C). The linear polymer degrades earlier compared to the crosslinked materials. The onset of mass loss, as indicated by $T_{5\%}$, was shifted from 257 °C down to 226 °C for the crosslinked materials.

diluents and one bifunctional crosslinker were synthesized and tested regarding their photoreactivity using a photobase generator (PBG). Promising results were obtained from photo-DSC experiments upon irradiation through high molecular weights and crosslinked materials. The monosubstituted Ar-C was proven to be the most efficient and reactive monomer, with the disadvantage of being thermally initiated with the PBG used in this study. Reactivity was significantly boosted from 100 °C on for Ar-C and slightly for Et-C but transitioned into an equilibrium of polymerization and depolymerization between 100 and 120 °C. Efficient network formation could be achieved for formulations of bifunctional Di-C containing 16–63 mol% Et-C. The resulting mechanical properties of obtained pure polycarbonate networks are highly tuneable from elastomeric behavior with reactive diluent amounts from about 50 mol% upwards to stiff, tough materials with crosslinker amounts above 50 mol%. This versatility in combination with the materials' potential to be biocompatible and biodegradable make the investigated monomers a highly interesting material platform, e.g. for medical applications. Furthermore, technological and chemical developments could soon make them accessible for Hot Lithography: Enhanced printing technology capable of higher printing temperatures is underway. Furthermore, screening of various photobase generators with varying counterions may lead to more reactive yet thermally stable formulations. [40] For example, phosphazene-based photobase generators are currently widely investigated. [48–51] Most commonly used as salt-based photobases, [49–51] they could also increase formulations' thermal stability in preventing premature gelation.

Declaration of Competing Interest

The authors declare that they have no known competing financial interests or personal relationships that could have appeared to influence the work reported in this paper.

Data availability

Data will be made available on request.

Appendix A. Supplementary data

Supplementary data to this article can be found online at https://doi.org/10.1016/j.reactfunctpolym.2022.105460.

References

[1] E. Quaranta, D. Sgherza, G. Tartaro, Depolymerization of poly(bisphenol A carbonate) under mild conditions by solvent-free alcoholysis catalyzed by 1,8-diazabicyclo[5.4.0]undec-7-ene as a recyclable organocatalyst: a route to chemical recycling of waste polycarbonate, Green Chem. vol. 19 (22) (2017) 5422–5434.
[2] T. Endo, General Mechanisms in Ring-Opening Polymerization, Handbook of Ring-Opening Polymerization, 2009, pp. 53–63.
[3] S. Sarel, L.A. Pohoryles, The stereochemistry and mechanism of reversible polymerization of 2,2-Disubstituted 1,3-Propanediol carbonates, J. Am. Chem. Soc. 80 (17) (1958) 4596–4599.
[4] J. Guo, M. Liu, Y. Gu, Y. Wang, J. Gao, F. Liu, Efficient alcoholysis of polycarbonate catalyzed by recyclable Lewis acidic ionic liquids, Ind. Eng. Chem. Res. 57 (32) (2018) 10915–10921.
[5] C. Tsutsumi, K. Yamamoto, A. Ichimaru, M. Nodono, K. Nakagawa, H. Yasuda, Biodegradations of block copolymers composed of l-or d, l-lactide and six-membered cyclic carbonates prepared with organolanthanide initiators, J. Polym. Sci. A Polym. Chem. 41 (22) (2003) 3572–3588.
[6] H.R. Kricheldorf, J. Jenssen, Polylactones., 16. Cationic polymerization of Trimethylene carbonate and other cyclic carbonates, J. Macromol. Sci. A Chem. 26 (4) (1989) 631–644.
[7] D.J. Darensbourg, A.I. Moncada, S.J. Wilson, Ring-opening polymerization of renewable six-membered cyclic carbonates. Monomer synthesis and catalysis, Green Polymer. Methods, 163–200.
[8] K.K. Yu, I. Curcic, J. Gabriel, H. Morganstewart, S.C. Tsang, Catalytic coupling of CO2 with epoxide over supported and unsupported amines, J. Phys. Chem. A 114 (11) (2010) 3863–3872.
[9] D.J. Darensbourg, S.J. Lewis, J.L. Rodgers, J.C. Yarbrough, Carbon dioxide/epoxide coupling reactions utilizing Lewis base adducts of zinc halides as catalysts. Cyclic carbonate versus polycarbonate production, Inorg. Chem. 42 (2) (2003) 581–589.
[10] L. Lu, X. Zhu, R.G. Valenzuela, B.L. Currier, M.J. Yaszemski, Biodegradable polymer scaffolds for cartilage tissue engineering, Clin. Orthop. Relat. Res. 391 (2001) S251–S270.
[11] A. Welle, M. Kröger, M. Döring, K. Niederer, E. Pindel, I.S. Chronakis, Electrospun aliphatic polycarbonates as tailored tissue scaffold materials, Biomaterials 28 (13) (2007) 2211–2219.
[12] W. Guo, V. Laserna, J. Rintjema, A.W. Kleij, Catalytic one-pot oxetane to carbamate conversions: formal synthesis of drug relevant molecules, Adv. Synth. Catal. 358 (10) (2016) 1602–1607.
[13] A. Dominski, T. Konieczny, K. Duale, M. Krawczyk, G. Pastuch-Gawołek, P. Kurcok, Stimuli-responsive aliphatic polycarbonate nanocarriers for tumor-targeted drug delivery, Polymers 12 (12) (2020) 2890.
[14] J. Sun, W. Birnbaum, J. Anderski, M.-T. Picker, D. Mulac, K. Langer, D. Kuckling, Use of light-degradable aliphatic polycarbonate nanoparticles as drug carrier for photosensitizer, Biomacromolecules 19 (12) (2018) 4677–4690.
[15] Z. Guo, E. Liang, J. Sui, M. Ma, L. Yang, J. Wang, J. Hu, Y. Sun, Y. Fan, Lapatinib-loaded acidity-triggered charge switchable polycarbonate-doxorubicin conjugate micelles for synergistic breast cancer chemotherapy, Acta Biomater. 118 (2020) 182–195.
[16] J. Feng, R.-X. Zhuo, X.-Z. Zhang, Construction of functional aliphatic polycarbonates for biomedical applications, Prog. Polym. Sci. 37 (2) (2012) 211–236.
[17] G. Hua, P. Olsén, J. Franzén, K. Odelius, Anionic polycondensation and equilibrium driven monomer formation of cyclic aliphatic carbonates, RSC Adv. 8 (68) (2018) 39022–39028.
[18] T. Ariga, T. Takata, T. Endo, Cationic ring-opening polymerization of cyclic carbonates with alkyl halides to yield polycarbonate without the ether unit by suppression of elimination of carbon dioxide, Macromolecules 30 (4) (1997) 737–744.
[19] T. Endo, Y. Shibasaki, F. Sanda, Controlled ring-opening polymerization of cyclic carbonates and lactones by an activated monomer mechanism, J. Polym. Sci. A Polym. Chem. 40 (13) (2002) 2190–2198.
[20] H. Yasuda, M.-S. Aludin, N. Kitamura, M. Tanabe, H. Sirahama, Syntheses and physical properties of novel optically active poly (ester– carbonate) s by copolymerization of substituted Trimethylene carbonate with ε-caprolactone and their biodegradation behavior, Macromolecules 32 (19) (1999) 6047–6057.
[21] D.M. Knauss, J.E. McGrath, Polycarbonate networks. 1. Synthesis and characterization of vinylphenylcarbonate terminated oligomers, Polymer 43 (24) (2002) 6407–6414.
[22] A.M. Schenzel, N. Moszner, C. Barner-Kowollik, Self-reporting dynamic covalent polycarbonate networks, Polym. Chem. 8 (2) (2017) 414–420.
[23] P.-L. Durand, G. Chollet, E. Grau, H. Cramail, Versatile cross-linked fatty acid-based polycarbonate networks obtained by thiol–ene coupling reaction, RSC Adv. 9 (1) (2019) 145–150.
[24] L.A. Link, A.T. Lonnecker, K. Hearon, C.A. Maher, J.E. Raymond, K.L. Wooley, Photo-cross-linked poly(thioether-co-carbonate) networks derived from the natural product Quinic acid, ACS Appl. Mater. Interfaces 6 (20) (2014) 17370–17375.
[25] D.I. Shiman, I.V. Vasilenko, S.V. Kostjuk, Cationic polymerization of isobutylene by complexes of alkylaluminum dichlorides with diisopropyl ether: an activating effect of water, J. Polym. Sci. A Polym. Chem. 52 (16) (2014) 2386–2393.
[26] E.W.P. Tan, J.L. Hedrick, P.L. Arrechea, T. Erdmann, V. Kiyek, S. Lottier, Y.Y. Yang, N.H. Park, Overcoming barriers in polycarbonate synthesis: a streamlined approach for the synthesis of cyclic carbonate monomers, Macromolecules 54 (4) (2021) 1767–1774.

[27] J.V. Crivello, J. Lam, Photoinitiated cationic polymerization with triarylsulfonium salts, J. Poly. Sci.: Poly. Chem. Ed. 17 (4) (1979) 977–999.
[28] H. Matsukizono, T. Endo, Mono- and bifunctional six-membered cyclic carbonates synthesized by diphenyl carbonate toward networked polycarbonate films, J. Appl. Polym. Sci. 132 (19) (2015) n/a–n/a.
[29] F. Nederberg, B.G.G. Lohmeijer, F. Leibfarth, R.C. Pratt, J. Choi, A.P. Dove, R. M. Waymouth, J.L. Hedrick, Organocatalytic ring opening polymerization of Trimethylene carbonate, Biomacromolecules 8 (1) (2007) 153–160.
[30] I.A. Barker, A.P. Dove, Triarylsulfonium hexafluorophosphate salts as photoactivated acidic catalysts for ring-opening polymerisation, Chem. Commun. 49 (12) (2013) 1205–1207.
[31] I. Jiménez-Pardo, L.G.J. van der Ven, R.A.T.M. van Benthem, A.C.C. Esteves, G. de With, Effect of a set of acids and polymerization conditions on the architecture of polycarbonates obtained via ring opening polymerization, J. Polym. Sci. A Polym. Chem. 55 (9) (2017) 1502–1511.
[32] J. Matsuo, K. Aoki, F. Sanda, T. Endo, Substituent effect on the anionic equilibrium polymerization of six-membered cyclic carbonates, Macromolecules 31 (14) (1998) 4432–4438.
[33] X. Li, N. Mignard, M. Taha, C. Fernández-de-Alba, J. Chen, S. Zhang, L. Fort, F. Becquart, Synthesis of poly(trimethylene carbonate) oligomers by ring-opening polymerization in bulk, Macromol. Chem. Phys. 221 (5) (2020) 1900367.
[34] B. Steyrer, B. Busetti, G. Harakály, R. Liska, J. Stampfl, Hot lithography vs. room temperature DLP 3D-printing of a dimethacrylate, Add. Manufact. 21 (2018) 209–214.
[35] C. Dall'Argine, A. Hochwallner, N. Klikovits, R. Liska, J. Stampf, M. Sangermano, Hot-lithography SLA-3D printing of epoxy resin, Macromol. Mater. Eng. 305 (10) (2020) 2000325.
[36] L. Pezzana, R. Wolff, G. Melilli, N. Guigo, N. Sbirrazzuoli, J. Stampfl, R. Liska, M. Sangermano, Hot-lithography 3D printing of biobased epoxy resins, Polymer 254 (2022), 125097.
[37] N. Klikovits, L. Sinawehl, P. Knaack, T. Koch, J. Stampfl, C. Gorsche, R. Liska, UV-induced cationic ring-opening polymerization of 2-Oxazolines for hot lithography, ACS Macro Lett. 9 (4) (2020) 546–551.
[38] Y. Mete, K. Seidler, C. Gorsche, T. Koch, P. Knaack, R. Liska, Cationic photopolymerization of cyclic esters at elevated temperatures and their application in hot lithography, Poly. Intern. 71 (2022) 1062–1071.
[39] H. Salmi, X. Allonas, C. Ley, A. Defoin, A. Ak, Quaternary ammonium salts of phenylglyoxylic acid as photobase generators for thiol-promoted epoxide photopolymerization, Polym. Chem. 5 (22) (2014) 6577–6583.
[40] N. Zivic, P.K. Kuroishi, F. Dumur, D. Gigmes, A.P. Dove, H. Sardon, Recent advances and challenges in the design of organic photoacid and photobase generators for polymerizations, Angew. Chem. Int. Ed. 58 (31) (2019) 10410–10422.
[41] K. Arimitsu, R. Endo, Application to photoreactive materials of photochemical generation of superbases with high efficiency based on photodecarboxylation reactions, Chem. Mater. 25 (22) (2013) 4461–4463.
[42] J.-X. Li, L. Liu, A.-H. Liu, Study on synthesis and photoactivity of N-substituted diazabicyclononane derivatives with different substituents, Int. J. Adhes. Adhes. 57 (2015) 118–124.
[43] D.J. Bergmann, E.M. Campi, W.R. Jackson, Q.J. McCubbin, A.F. Patti, Rhodium-catalysed hydroformylation and carbonylation of N-alkenyl-1, 3-diaminopropanes, Tetrahedron 53 (51) (1997) 17449–17460.
[44] K. Studer, K. Dietliker, T. Jung, Photolatent amidine bases for redox curing of radically curable formulations, WO2009095282A2 (2009).
[45] E. Din, 527–2 DIN EN ISO 527-2: 2012–06, Kunststoffe–Bestimmung der Zugeigenschaften–Teil 2: Prüfbedingungen für Form-und Extrusionsmassen, Beuth Verlag, Deutsche Fassung, Berlin, 2012.
[46] J.L. Hedrick, V. Piunova, N.H. Park, T. Erdmann, P.L. Arrechea, Simple and efficient synthesis of functionalized cyclic carbonate monomers using carbon dioxide, ACS Macro Lett. 11 (3) (2022) 368–375.
[47] T.M. McGuire, E.M. López-Vidal, G.L. Gregory, A. Buchard, Synthesis of 5- to 8-membered cyclic carbonates from diols and CO2: a one-step, atmospheric pressure and ambient temperature procedure, J. CO2 Utiliz. 27 (2018) 283–288.
[48] S. Boileau, N. Illy, Activation in anionic polymerization: why phosphazene bases are very exciting promoters, Prog. Polym. Sci. 36 (9) (2011) 1132–1151.
[49] H. Yang, Y. Zuo, J. Zhang, Y. Song, W. Huang, X. Xue, Q. Jiang, A. Sun, B. Jiang, Phosphazene-catalyzed oxa-Michael addition click polymerization, Polym. Chem. 9 (38) (2018) 4716–4723.
[50] V. Puchelle, H. Du, N. Illy, P. Guégan, Polymerization of epoxide monomers promoted by tBuP4 phosphazene base: a comparative study of kinetic behavior, Polym. Chem. 11 (21) (2020) 3585–3592.
[51] D. Jardel, C. Davies, F. Peruch, S. Massip, B. Bibal, Protonated Phosphazenes: structures and hydrogen-bonding Organocatalysts for carbonyl bond activation, Adv. Synth. Catal. 358 (7) (2016) 1110–1118.